14-3-3 binding to LRRK2 is disrupted by multiple Parkinson's disease associated mutations and regulates cytoplasmic localisation

Jeremy Nichols, Nicolas Dzamko, Nicholas A Morrice, David G Campbell, Maria Deak, Alban Ordureau, Thomas Macartney, Youren Tong, Jie Shen, Alan Prescott, et al.

14-3-3 binding to LRRK2 is disrupted by multiple Parkinson's disease associated mutations and regulates cytoplasmic localisation

By

R. Jeremy Nichols[1,4], Nicolas Dzamko[1], Nicholas A. Morrice[1,5], David G. Campbell[1], Maria Deak[1], Alban Ordureau[1],Thomas Macartney[1], Youren Tong[3], Jie Shen[3], Alan R. Prescott[2] and Dario R. Alessi[1]

MRC Protein Phosphorylation Unit, College of Life Sciences, University of Dundee, Dow Street, Dundee DD1 5EH, Scotland.

Division of Cell Biology and Immunology, College of Life Sciences, University of Dundee, Dow Street, Dundee DD1 5EH, Scotland.

Center for Neurologic Diseases, Brigham and Women's Hospital, Program in Neuroscience, Harvard Medical School, Boston, MA 02115.

Present address: Parkinson's Institute, 675 Almanor Ave, Sunnyvale CA, 94085

Present address: The Beatson Institute for Cancer Research, Garescube estate, Switchback Road, Bearsden, Glasgow, G61 1BD

Correspondence to RJN (jnichols@parkinsonsinstitute.org) or DRA (d.r.alessi@dundee.ac.uk)

Tel +44 1382 385602
Fax +44 1382 223778

Short Title: Characterisation of interaction of LRRK2 with 14-3-3

Abstract The Leucine-Rich Repeat Protein Kinase 2 (LRRK2) is mutated in a significant number of Parkinson's disease patients, but still little is understood about how it is regulated or functions. Here we demonstrate that 14-3-3 isoforms interact with LRRK2. Consistent with this, endogenous LRRK2 isolated from Swiss 3T3 cells or various mouse tissues is associated with endogenous 14-3-3 isoforms. We also establish that 14-3-3 binding is mediated by phosphorylation of LRRK2 at two conserved residues (Ser910 and Ser935) located before the leucine-rich repeat domain. Our data suggests that mutation of Ser910 and/or Ser935 to disrupt 14-3-3 binding does not affect intrinsic protein kinase activity but induces LRRK2 to accumulate within discrete cytoplasmic pools perhaps resembling inclusion bodies. To investigate links between 14-3-3 binding and Parkinson's disease, we studied how 41 reported mutations of LRRK2 affected 14-3-3 binding and cellular localisation. Strikingly, we find that five of the six most common pathogenic mutations (R1441C, R1441G, R1441H, Y1699C, I2020T) display markedly reduced phosphorylation of Ser910/Ser935 thereby disrupting interaction with 14-3-3. We also demonstrate that Ser910/Ser935 phosphorylation and 14-3-3 binding to endogenous LRRK2 is significantly reduced in tissues of homozygous LRRK2[R1441C] knockin mice. Consistent with 14-3-3 regulating localisation, all of the common pathogenic mutations displaying reduced 14-3-3-binding, accumulated within inclusion bodies. We also found that three of the 41 LRRK2 mutations analysed displayed elevated protein kinase activity (R1728H ~2-fold, G2019S ~3-fold and T2031S ~4-fold). These data provide the first evidence suggesting that 14-3-3 regulates LRRK2 and that disrupting interaction of LRRK2 with 14-3-3 may be linked to Parkinson's disease.

Introduction

Autosomal dominant missense mutations within the gene encoding for the Leucine-Rich Repeat protein Kinase 2 (LRRK2) predispose humans to develop Parkinson's disease (PD)[1, 2]. LRRK2 is a large enzyme (2527 residues), consisting of leucine-rich repeats (residues 1010-1287), GTPase domain (residues 1335-1504), COR domain (residues 1517-1843), serine/threonine protein kinase domain (residues 1875-2132) and a WD40 repeat (residues 2231-2276) [3]. Patients with LRRK2 mutations generally develop PD with clinical symptoms indistinguishable from idiopathic PD at around 60-70 years of age [4]. Mutations in LRRK2 account for 4% of familial PD, and are observed in 1% of sporadic PD patients [4]. Over 40 missense mutations have been reported that are scattered throughout LRRK2 [5, 6].

The activity as well as localisation of a subset of mutant forms of LRRK2 has been analysed in previous work using various forms of recombinant LRRK2 expressed and assayed using diverse approaches [3, 7]. This has revealed that the most frequent mutation comprising an amino acid substitution of the highly conserved Gly2019 located within the subdomain VII-DFG motif of the kinase domain, enhances protein kinase activity around two-fold [8-10], suggesting LRRK2 kinase inhibitors might be useful for the treatment of PD. It was also reported that various mutants such as LRRK2[R1441C] and LRRK2[Y1699C] accumulated within discrete cytosolic pools resembling inclusion bodies that were suggested to consist of aggregates of misfolded protein [9].

In this study we demonstrate that endogenous LRRK2 interacts with endogenous 14-3-3 isoforms and that this binding is mediated via phosphorylation of LRRK2 at Ser910 and Ser935. We provide evidence that disruption of 14-3-3-binding induces LRRK2 to accumulate within cytoplasmic pools, similar in appearance to those reported previously for the LRRK2[R1441C] and LRRK2[Y1699C] mutants. Comparing the properties of 41 Parkinson's disease associated mutant forms of LRRK2 strikingly revealed that ten of these displayed markedly reduced phosphorylation of Ser910/Ser935 and 14-3-3 binding that included five common well characterised pathogenic mutations (R1441C, R1441G, R1441H, Y1699C, I2020T). We also observed that most mutants displaying reduced Ser910/Ser935 phosphorylation and association with 14-3-3, accumulated within cytoplasmic pools. These results provide the first evidence that a significant number of Parkinson's disease associated mutations inhibit Ser910/Ser935 phosphorylation, disrupting 14-3-3 binding and leading to accumulation of LRRK2 within cytoplasmic pools. Our study will stimulate further work to explore whether disruption of 14-3-3 binding to LRRK2 is linked to the development of Parkinson's disease.

Materials and Methods

Reagents and General methods. Tissue-culture reagents were from Life Technologies. P81 phosphocellulose paper was from Whatman and [γ-^{32}P]-ATP was from Perkin Elmer. All peptides were synthesised by Pepceuticals. The Flp-in T-REx system was from Invitrogen and stable cell lines, generated as per manufacturer instructions by selection with hygromycin, have been described previously [11]. Restriction enzyme digests, DNA ligations and other recombinant DNA procedures were performed using standard protocols. All mutagenesis was carried out using the Quick-Change site-directed-mutagenesis kit (Stratagene). DNA constructs used for transfection were purified from Escherichia coli DH5α using Qiagen or Invitrogen plasmid Maxi kits according to the manufacturer's protocol. All DNA constructs were verified by DNA sequencing, which was performed by The Sequencing Service, School of Life Sciences, University of Dundee, Scotland, U.K., using DYEnamic ET terminator chemistry (Amersham Biosciences) on Applied Biosystems automated DNA sequencers.

Buffers. Lysis Buffer contained 50 mM Tris/HCl, pH 7.5, 1 mM EGTA, 1 mM EDTA, 1% (w/v) 1 mM sodium orthovanadate, 10 mM sodium β-glycerophosphate, 50 mM NaF, 5 mM sodium pyrophosphate, 0.27 M sucrose, 1 mM Benzamidine and 2 mM phenylmethanesulphonylfluoride (PMSF) and was supplemented with 1% Triton X-100. Buffer A contained 50 mM Tris/HCl, pH 7.5, 50 mM NaCl, 0.1 mM EGTA and 0.27 M sucrose. Lambda phosphatase reactions were carried out in buffer A supplemented with 1mM $MnCl_2$, 2 mM DTT and 0.5 μg lambda phosphatase.

Antibodies. Anti-LRRK2 100-500 (S348C and S406C) and Anti-LRRK2 2498-2514 (S374C) were described previously [8]. Antibody against LRRK2 phosphoserine 910 (S357C) was generated by injection of the KLH conjugated phosphopeptide VKKKSNpSISVGEFY (where pS is phosphoserine) into sheep and was affinity purified by positive and negative selection against the phospho and de-phospho peptides respectively. Antibody against LRRK2 phosphoserine 935 (S814C) was generated by injection of the KLH conjugated phosphopeptide NLQRHSNpSLGPIFDH (where pS is phosphoserine) into sheep and was affinity purified by positive and negative selection against the phospho and de-phospho peptides respectively. Anti GFP antibody (S268B) was raised against recombinant GFP protein and affinity purified against the antigen. Anti-FLAG M2 antibody and affinity matrix were from Sigma (A2220). Nanotrap GFP binder affinity matrix was from ChromoTek. Rabbit polyclonal antibody recognizing 14-3-3 (K-19, SC-629) and control rabbit IgG (SC-2027) antibody were from SantaCruz biotechnology. HSP90 antibody was from Cell signaling technology (#4877). Anti-MARK3 was from Upstate (#05-680).

Cell culture, treatments and cell lysis. HEK-293 and Swiss 3T3 cells were cultured in Dulbecco's Modified Eagle's medium supplemented with 10% FBS, 2mM glutamine and 1×antimycotic/antibiotic solution. HEK-293 T-REx cell lines were cultured in DMEM supplemented with 10% FBS and 2mM glutamine, 1X antimycotic/antibiotic, and 15 μg/ml Blastocidin and 100 μg/ml hygromycin. Cell transfections were performed by the polyethylenimine method [12]. T-Rex cultures were induced to express the indicated protein by inclusion of 1 μg/ml doxycycline in the culture medium for 24 hours. Per 15cm dish, cells washed once with PBS and lysed in situ with 1.0 ml of lysis buffer, on ice, then centrifuged at 16,000 x g at 4 °C for 10 minutes. Protein concentrations were determined using the Bradford method with BSA as the standard

SILAC media. SILAC DMEM (high glucose without $NaHCO_3$, L-glutamine, arginine, lysine and methionine Biosera #A0347) was prepared with 10% dialyzed FBS (Hyclone) and supplemented with methionine, glutamine, $NaHCO_3$, labeled or unlabeled arginine and lysine. Cells harbouring GFP tagged proteins were cultured in SILAC DMEM for three passages at a 1:10 ratio with the following isotopic labelling. For GFP versus wild type LRRK2, L-arginine (84 µg/ml; Sigma-Aldrich) and L-lysine (146 µg/ml lysine; Sigma-Aldrich) were added to the GFP "light" media, while L-arginine ^{13}C and L-lysine ^{13}C (Cambridge Isotope Laboratory) were added to the GFP-LRRK2 wild type "heavy" media at the same concentrations. For GFP versus LRRK2 G2019S experiments, L-arginine and L-lysine were added to the GFP "light" media and L-arginine $^{13}C/^{15}N$ and L-lysine $^{13}C/^{15}N$ (Cambridge Isotope Laboratory) to the GFP-LRRK2 G2019S "heavy" media. The amino acid concentrations are based on the formula for normal DMEM (Invitrogen). Once prepared, the SILAC media was mixed well, filtered through a 0.22-µm filter (Millipore). Metabolically labeled cells were induced to express GFP or the GFP-LRRK2 fusion protein for 24 hours by inclusion of doxycycline in the culture media.

SILAC labelling and Mass spectrometry. Cells metabolically labeled and induced to express either GFP or LRRK2-wild type or G2019S were lysed in lysis buffer supplemented with 1% Triton X-100 at 0.5 ml per 10 cm dish. For each condition individually, 9 mg of cell lysate was subjected to individual immunoprecipitation with a 20µl bed volume of GFP binder agarose beads for 1 hour at 4°C. Beads were washed once with 5ml and then with 10 ml of lysis buffer supplemented with 1% Triton-X 100 and 300 mM NaCl. Beads were then washed once with 5 ml and then once with 10 ml storage buffer. Bead associated proteins were eluted with 1X LDS sample buffer for 10 min at 70°C then passed through a 0.22 µm spin-X column. Control GFP eluates were combined with either eluates of wild type LRRK2 or LRRK2 G2019S in equal amounts and reduced and alkylated as above. Samples were resolved on a 12% Novex gel for only one half of the gel. Gels were stained with colloidal blue overnight and destained for 3 hours. The entire lane was excised in 9 total bands and digested with trypsin as described previously [13]. The digests were separated on a Biosphere C_{18} trap column (0.1 mm id x 2 mm, Nanoseparations, Holland) connected to a PepMap C18 nano column (75 µm x 15 cm, Dionex Corporation) fitted to a Proxeon Easy-LC nanoflow LC-system (Proxeon, Denmark) with solvent A (2% acetonitrile/0.1% formic acid/98% water) and solvent B (90% acetonitrile/10% water/0.09% formic acid). 10 µl of sample (a total of 2 µg of protein) was loaded with a constant flow of 7 µl/min onto the trap column in solvent A and washed for 3 min at the same flow rate. After trap enrichment, peptides were eluted with a linear gradient of 5-50% solvent B over 90 min with a constant flow of 300 nl/min. The HPLC system was coupled to a linear ion trap-orbitrap hybrid mass spectrometer (LTQ-Orbitrap XL, Thermo Fisher Scientific Inc) via a nanoelectrospray ion source (Proxeon Biosystems) fitted with a 5cm Picotip FS360-20-10 emitter. The spray voltage was set to 1.2 kV and the temperature of the heated capillary was set to 200°C. Full scan MS survey spectra (m/z 350-1800) in profile mode were acquired in the Orbitrap with a resolution of 60,000 after accumulation of 500,000 ions. The five most intense peptide ions from the preview scan in the Orbitrap were fragmented by collision-induced dissociation (normalized collision energy 35%, activation Q 0.250 and activation time 30 ms) in the LTQ after the accumulation of 10,000 ions. Maximal filling times were 1,000 ms for the full scans and 150 ms for the MS/MS scans. Precursor ion charge state screening was enabled and all unassigned charge states as well as singly charged species were rejected. The lock mass option was enabled for survey scans to improve mass accuracy. Data were acquired using the Xcalibur software.

LC-MS Data Analysis using MaxQuant. The raw mass spectrometric data files obtained for each experiment was collated into a single quantitated dataset using MaxQuant (version 1.0.13.13) (http://www.maxquant.org) and the Mascot search engine (Matrix Science, version 2.2.2) software. Enzyme specificity was set to that of trypsin. Other parameters used within the software: Variable modifications- Methionine Oxidation; Database- target-decoy human MaxQuant (ipi.HUMAN.v3.52.decoy) (containing 148,380 database entries); Labels- R6K4 [for GFP versus wild type LRRK2] or R10K8 [for GFP versus LRRK2 G2019S]; MS/MS tolerance- 0.5 Da; (e) Top MS/MS peaks per 100 Da- 5; Maximum missed cleavages- 2; Maximum of labeled amino-acids was 3; False Discovery Rate (FDR) was 1%.

Phosphorylation site identification by mass spectrometry. Endogenous and recombinant LRRK2 was immunoprecipitated from 50 mg of Swiss 3T3 lysate or T-Rex cells induced to express FLAG-LRRK2 cell lysate using anti –LRRK2 (100-500) or anti-FLAG agarose, respectively. Immunoprecipitates were eluted from the affinity matrices using 2X LDS sample buffer or 200 μg/ml FLAG peptide then filtered through a 0.2 μm Spin-X column (Corning) before reduction with 10mM dithiothretol and alkylation with 50 mM iodoacetamide. Samples were heated for 10 min at 70 °C and resolved on 4-12% Novex gels before staining with colloidal blue (Invitrogen). Bands corresponding to LRRK2 were excised and digested with trypsin as described previously [16]. Samples were analyzed on an LTQ Orbitrap XL mass spectrometer (Thermo) as described above, except the top 5 ions were fragmented in the linear ion trap using multistage activation of the neutral loss of phosphoric acid from the parent ion (neutral loss masses = 49, 32.33 and 24.5 for z= 2,3 and 4). Mascot generic files were created from the raw files using raw2msm (gift from M.Mann) and were searched on a local Mascot server (matrixscience.com) using the International Protein Index (IPI) mouse database for endogenous LRRK2 or the IPI human database for recombinant LRRK2.

Immunological procedures. Cell lysates (10-30 μg) were resolved by electrophoresis on SDS polyacrylamide gels or Novex 4-12% gradient gels, and electroblotted to nitrocellulose membranes. Membranes were blocked with 5% skimmed milk (w/v) in 50 mM Tris/HCl, pH 7.5, 0.15 M NaCl and 0.1% (v/v) Tween (TBST Buffer). For phospho- antibodies, primary antibody was used at a concentration of 1 μg/ml, diluted in 5% skimmed milk in TBST with the inclusion of 10 μg/ml dephosphorylated-peptide. All other antibodies were used at 1 μg/ml in 5% (w/v) milk in TBST. Detection of immune-complexes was performed using either flourophore conjugated secondary antibodies (Molecular Probes) followed by visualisation using an Odyssey LICOR or by horseradish-peroxidase-conjugated secondary antibodies (Pierce) and an enhanced-chemiluminescence reagent. For immunoprecipitations, antibody was non-covalently coupled to protein G-Sepharose at a ratio of 1 μg antibody/μl of beads, or anti-FLAG M2-agarose was utilized. Cell lysate was incubated with coupled antibody for 1 hour. To assess Ser935 phosphorylation, total LRRK2 levels and 14-3-3 binding in mouse tissues, LRRK2 was immunoprecipitated from 6 mg of whole tissue lysate using 15 μg antibody coupled to 15 μl of Protein G-Sepharose. Ser910 phosphorylation was assessed following immunoprecipitation from 10 mg of tissue lysate. Immune complexes were washed twice with lysis buffer supplemented with 0.3 M NaCl and twice with Buffer A. Precipitates were re-suspended in LDS sample Buffer and subjected to immunoblot analysis. Digoxigenen (DIG) labelled 14-3-3 for use in overlay far western analysis was prepared as described in [14]. To directly assess 14-3-3 interaction with LRRK2, immunoprecipitates were electroblotted to nitrocellulose membranes and blocked with 5% skimmed milk for 30 minutes. After washing with TBST, membranes were incubated with DIG labelled 14-3-3

diluted to 1μg/ml in 5% BSA in TBST overnight at 4°C. DIG 14-3-3 was detected with HRP labelled anti-DIG Fab fragments (Roche).

LRRK2 Immunoprecipitation Kinase assays. 500 μg of transfected cell lysates was subjected to immunoprecipitation with 5 μl bed volume of anti-FLAG agarose for 1 hr. Beads were washed twice with Lysis Buffer supplemented with 300 mM NaCl, the twice with Buffer A. Peptide Kinase Assays were set up in a total volume of 50 μl with immunoprecipitated LRRK2 in 50 mM Tris pH 7.5, 0.1 mM EGTA, 10 mM $MgCl_2$ and 0.1 mM [γ-^{32}P]ATP (~300-500 cpm/pmol) in the presence of 200 μM long variant of the LRRKtide peptide substrate (RLGRDKYKTLRQIRQGNTKQR) [10, 11] or the Nictide peptide substrate (RLGWWRFYTLRRARQGNTKQR) [11]. Reactions were terminated by applying 30 μl of the reaction mixture on to P81 phosphocellulose paper and immersion in 50 mM phosphoric acid. After extensive washing, reaction products were quantitated by Cerenkov counting. One half of the remaining reaction was subjected to immunoblot analysis using the Odyssey LICOR system and specific activity is represented as cpm/LICOR independent density values.

Affinity purification of 14-3-3 with a di-phosphorylated peptide encompassing Ser910 and Ser935. An N-terminally biotinylated di-phosphorylated peptide encompassing Ser910 and Ser935 (biotin-KKKSN[pS]ISVGEFYRDAVLQRCSPNLQRHSN[pS]LGPIF) was conjugated to streptavidin agarose (1 μg peptide per μg of Agarose). Aliquots of agarose beads (10 μl) were treated with or without lambda phosphatase for 30 min at 30°C, with lambda phosphatase being in the presence or absence of 50 mM EDTA. Conjugated beads were then incubated with 3 mg of HEK 293 cell lysate at 4°C for 1h. Following two washes with lysis buffer supplemented with 0.5 M NaCl beads were boiled in LDS sample buffer and samples subjected to immunoblot analysis for 14-3-3.

Fluorescence Microscopy. HEK-293 Flp-in T-REx cells harbouring GFP tagged LRRK2 and PD associated mutations were plated in 4-well glass bottom, CC2 coated chamber slides (Nunc). One day after plating, cells were induced with 1 μg/ml doxycycline and 24hr later, cells were fixed in 4% paraformaldehyde buffered in phosphate buffered saline (purchased from USB, # 19943). Cells were mounted in ProLong Gold (Invitrogen) and imaged under the same settings for each mutant, on a Zeiss LSM 700 confocal microscope using an α Plan-Apochromat x100 objective.

Results

Association of LRRK2 with 14-3-3. We employed quantitative Stable Isotope Labelling with Amino acids in Cell culture (SILAC)-based mass spectrometry to identify proteins associated with immunoprecipitates of stably expressed full length GFP-LRRK2 (Fig 1A) as well as the GFP-LRRK2[G2019S] mutant (Fig 1B) derived from HEK-293 cells. The top hits, that were enriched at 10 to 30-fold higher levels with GFP-LRRK2 or GFP-LRRK2[G2019S] compared to GFP alone, comprised various isoforms of 14-3-3 (Fig 1). The two other major interactors observed were two isoforms of the heat shock protein-90 (Hsp90) chaperone-associated with its kinase-specific targeting CDC37 subunit (enriched 5 to 15-fold). Hsp90 and CDC37 associated with both wild type LRRK2 as well as LRRK2[G2019S] mutant and have previously been reported to interact with LRRK2 [15]. No other significant interactors of LRRK2 were detected in this screen.

We found that endogenous 14-3-3 as well as Hsp90, was co-immunoprecipitated with endogenous LRRK2 from Swiss 3T3 cells (Fig 2A). We also observed that endogenous LRRK2 was co-immunoprecipitated with an antibody that recognises endogenous 14-3-3 isoforms from Swiss 3T3 cells (Fig 2B). Plasmids encoding expression of seven isoforms of human 14-3-3 were transfected into HEK-293 cells stably expressing full length FLAG-LRRK2. Following affinity purification, apart from the atypical sigma isoform, all other isoforms of 14-3-3 interacted with FLAG-LRRK2 (Fig 2C). As a control we also demonstrate that all 14-3-3 isoforms except 14-3-3 sigma interacted with endogenous MAP/microtubule affinity regulating kinase-3 (MARK3), a previously characterised 14-3-3 interactor [16].

14-3-3 isoforms mostly interact with specific phosphorylated residues on their binding partners [17, 18]. To verify whether association of 14-3-3 with LRRK2 was dependent upon phosphorylation, we incubated endogenous LRRK2 (Fig 2D) or overexpressed FLAG-LRRK2 (Fig 2E) in the presence or absence of lambda phosphatase. Lambda phosphatase markedly reduced interaction of 14-3-3 with LRRK2 assessed using the overlay assay. This effect was suppressed by the inclusion of the lambda phosphatase inhibitor EDTA in the assay (Fig 2D & 2E). Residual binding of 14-3-3 to LRRK2 following lambda phosphatase treatment is presumably due incomplete dephosphorylation of LRRK2.

Mapping of major phosphorylation sites on endogenous LRRK2. To determine which phosphorylated residue(s) mediate binding to 14-3-3, we performed detailed phospho-peptide orbitrap mass spectrometry analysis of endogenous LRRK2 immunoprecipitated from mouse Swiss 3T3 cells (Fig 3A). This revealed three clear phosphorylation sites namely Ser860, Ser910 and Ser935 (Fig 3B). These residues lie in the N-terminal non-catalytic region of LRRK2 just prior to the leucine-rich repeats (Fig 3C). We also analysed phosphorylation of overexpressed full length human FLAG-LRRK2 expressed in HEK-293 cells, which confirmed that Ser860, Ser910 and Ser935 were major sites of phosphorylation (Fig 3A & 3B). In addition, we found three other phosphorylation sites in the overexpressed human FLAG-LRRK2 preparation namely Ser955, Ser973 and Ser976 (Fig 3B & 3C). The phospho-peptides encompassing Ser955, Ser973 and Ser976 were also detected in our analysis of endogenous LRRK2 but due to the lower abundance of these peptides we were unable to assign the exact phosphorylation sites (data not shown).

Phosphorylation of Ser910 and Ser935 mediates 14-3-3 binding, but does not control kinase activity. We observed that mutation to Ala of Ser860, Ser955, Ser973, Ser976 or both Ser973+976 phosphorylation sites, did not affect binding of 14-3-3 to full length FLAG-LRRK2 (Fig 3D). Strikingly however, mutation of Ser910 and/or Ser935 to Ala, abolished

14-3-3 interaction, indicating that phosphorylation of both of these residues is necessary for binding of LRRK2 to 14-3-3 isoforms (Fig 3D). Mutation of Ser910 and/or Ser935 or any of the other identified phosphorylation site did not affect LRRK2 protein kinase activity (Fig 3D). To study whether phosphorylation of Ser910 and Ser935 was sufficient to mediate interaction with 14-3-3 isoforms, we generated a di-phosphorylated biotinylated peptide encompassing Ser910 and Ser935. We observed that when this was conjugated to streptavidin-Agarose it efficiently affinity purified 14-3-3 isoforms from 293 cell extracts (Fig 3E). Incubation of this peptide with lambda phosphatase to dephosphorylate Ser910 and Ser935 prevented interaction with 14-3-3 isoforms, an effect that was not observed when the lambda phosphatase inhibitor EDTA was included (Fig 3E).

Generation of Ser910 and Ser935 phosphospecific antibodies. We next generated phosphospecific antibodies recognising LRRK2 phosphorylated at Ser910 or Ser935. These antibodies were specific, as mutation of Ser910 to Ala ablated recognition of LRRK2 with phospho-Ser910 antibody and similarly, mutation of Ser935 abolished recognition with the phospho-Ser935 antibody (Fig 3F). We consistently observed that mutation of Ser910 to Ala reduced phosphorylation of Ser935 about two-fold and vice versa mutation of Ser935 reduced phosphorylation of Ser910 around two-fold as quantitated by LICOR (Fig 3F). Utilising these antibodies, we demonstrate that endogenous LRRK2 immunoprecipitated from mouse brain, kidney and spleen was phosphorylated at Ser910 as well as Ser935 and also bound 14-3-3 (Fig 3G).

Sequence alignments indicate that the Ser910 and Ser935 sites as well as residues surrounding them are highly conserved in mammalian species (Fig 3H). This region encompassing Ser910 and Ser935 is not present in *Caenorhabditis elegans* or *Drosophila melanogaster* LRK-1, or indeed mammalian LRRK1. Comparison of the residues surrounding Ser910 and Ser935 indicates some striking similarities (Fig 3 I i.e. basic residues -3 and -4 positions, Ser residue at the -2 position, Asn at the -1 position and a large hydrophobic residue at the + 1 position).

Disruption of 14-3-3 binding induces accumulation of LRRK2 within cytoplasmic pools resembling inclusion bodies. A common role of 14-3-3 proteins is to influence the subcellular localisation of the protein to which it binds. We therefore studied whether 14-3-3 binding might affect LRRK2 cellular localisation. To ensure low level and as uniform as possible expression, we generated Flp-in T-REx 293 cells that stably express wild type and non-14-3-3-binding Ser910/Ser935 mutant forms of full-length GFP-LRRK2. Immunoblot analysis revealed that wild type and mutant GFP-LRRK2 forms were expressed at similar levels (Fig 4A). We next studied the cellular localisation using confocal microscopy and found, that consistent with a previous report [19], wild type LRRK2 was uniformly distributed throughout the cytosol and excluded from the nucleus (Fig 4B). In contrast, the non-14-3-3-binding LRRK2[S910A], LRRK2[S935A] and LRRK2[S910A+S935A] mutants accumulated within cytosolic pools resembling inclusion bodies (Fig 4B).

Characterisation of 14-3-3 binding of 41 LRRK2 disease associated mutants. We next decided to investigate the Ser910/Ser935 phosphorylation and 14-3-3 binding properties of 41 Parkinson's disease forms of LRRK2. These mutations include the six most common pathogenic mutations that have been described to date (R1441C, R1441G, R1441H, Y1699C, G2019S, I2020T) [5, 6]. Most of the other mutations studied have only been observed in low numbers of Parkinson's disease patients and further work is required to assess the contributions these mutation make to the development of disease [6]. The location of the

different mutations in LRRK2 analysed is indicated in the Figure 5 inset. We expressed full-length wild type and mutant forms of LRRK2 with an N-terminal Flag epitope tag in 293 cells. LRRK2 was immunoprecipitated and levels of protein determined by quantitative LICOR-immunoblotting analysis. Similar levels of LRRK2 forms were subjected to immunoblot analysis, which revealed that most of the mutants were phosphorylated at Ser910 and Ser935 to a similar extent as the wild type enzyme and interacted with 14-3-3 (Fig 5, lower panel). However, Ser910/Ser935 phosphorylation and hence 14-3-3 binding were abolished in four mutants (R1441G, Y1699C, E1874stop and I2020T) (Fig 5, lower panel). Phosphorylation of Ser910/Ser935 and 14-3-3 binding were significantly reduced in six other mutants (M712V, R1441H, R1441C, A1442P, L1795F and G2385R) (Fig 5, lower panel).

We also compared the relative protein kinase specific activity of the 41 mutant forms of LRRK2 employing the LRRKtide peptide substrate [10] (Fig 5). Consistent with previous work [8-10], LRRK2[G2019S] mutant possessed ~3-fold higher specific activity than wild type LRRK2. Two other mutants LRRK2[R1728H] and LRRK2[T2031S] also exhibited two and four-fold increased activity respectively than wild type LRRK2 . Apart from the R1874stop mutation that lacks the kinase domain and is therefore inactive, all other mutants tested possessed similar activity to wild type LRRK2.

Association of 14-3-3 with endogenous LRRK2 is impaired in LRRK2[R1441C] knockin mice. To obtain further evidence that the LRRK2[R144C] Parkinson's disease mutation disrupts 14-3-3 binding, we compared levels of 14-3-3 associated with endogenous LRRK2 derived from previously reported littermate wild type and homozygous LRRK2[R144C] knockin mice [20]. LRRK2 was immunoprecipitated from spleen, kidney and brain from three separate mice of each genotype. Immunoblotting and 14-3-3 overlay analysis demonstrated that level of LRRK2 expression was similar in the wild type and knock-in mice, however the level of Ser910/Ser935 phosphorylation and associated 14-3-3 was markedly reduced in tissues derived from LRRK2[R1441C] knock-in mice compared to wild type (Fig 6). The largest effect of the knock-in mutation was observed in kidney.

Cellular localisation of 41 mutant forms of LRRK2. To ensure low level and as uniform as possible expression of wild type and mutant forms of full length GFP-LRRK2, we generated the Flp-in T-REx 293 cells that stably express wild type and mutant forms of GFP-LRRK2. Immunoblot analysis revealed that GFP-LRRK2 forms were expressed at relatively similar levels (Fig 7). The localisation of wild type, kinase dead and many other LRRK2 mutants studied were uniformly distributed throughout the cytosol and excluded from the nucleus with no accumulation within cytoplasmic pools observed (Fig 7 or Supplementary Fig 1 to view larger images). Strikingly, most mutants that displayed reduced Ser910/Ser935 phosphorylation and binding to 14-3-3, accumulated within cytosolic pools resembling inclusion bodies (R1441C, R1441G, R1441H, A1442P, Y1699C, L1795F, I2020T). Not counting the truncated E1874stop mutant, which displays diffuse cytoplasmic localisation, only two other mutants (M712V and G2385R) displaying reduced Ser910/Ser935 phosphorylation and 14-3-3 binding (Fig 5) but did not accumulate in cytoplasmic pools (Fig 7 or Supplementary Fig 1). It is possible that the ability of these mutants to still interact weakly with 14-3-3 isoforms may prevent their accumulation within cytoplasmic pools. Only a single mutant (R1067Q) was found to interact with 14-3-3 and accumulate within cytoplasmic pools (Fig 7 or Supplementary Fig 1). The reasons for this require further work.

Discussion

In this study we establish that 14-3-3 isoforms interact with endogenous LRRK2 and this is mediated by phosphorylation of Ser910 and Ser935. The finding that a di-phosphorylated peptide encompassing Ser910 and Ser935 interacted with 14-3-3 isoforms in 293 cell extracts and that LRRK2 Ser910Ala/Ser935Ala do not interact with 14-3-3 suggests that phosphorylation of these residues is necessary and sufficient to enable LRRK2 to interact with 14-3-3 isoforms. 14-3-3 proteins interact dynamically with many intracellular proteins, exerting widespread influence on diverse cellular processes. They operate by binding to specific phosphorylated residues on target proteins. The finding that LRRK2 interacts with 14-3-3 isoforms could not be predicted by analysis of the primary sequence, because the residues surrounding the 910 and 935 phosphorylation sites do not adhere to the optimal Mode 1 and 2 consensus binding motifs for a common mode of 14-3-3 interaction [17, 18]. However, many proteins that interact with 14-3-3 do so via diverse non-predictable atypical binding motifs, presumably because other structural features contribute to the interactions [17].

Our data suggests that phosphorylation of both Ser910 and Ser935 is required for stable interaction of 14-3-3 with LRRK2, as mutation of either Ser910 or Ser935 abolishes 14-3-3 interaction. 14-3-3 molecules form dimers with each monomer having the ability to interact with a phosphorylated residue [18]. Thus, a 14-3-3 dimer has the capacity to interact with two phosphorylated residues. It is possible that one dimer of 14-3-3 interacts with both phosphorylated Ser910 and phosphorylated Ser935. We also observed that mutation of either Ser910 or Ser935 to an Ala residue induced a significant dephosphorylation of the other residue (Fig 3F). This could be explained if 14-3-3 binding protected Ser910 and Ser935 from becoming dephosphorylated by a protein phosphatase. Thus abolishing 14-3-3 binding by mutation of either Ser910 or Ser935 would promote dephosphorylation of the other site. 14-3-3 binding to other targets such as phosphatidylinositol 4-kinase III beta [21] or Cdc25C [22] protects these enzymes from dephosphorylation, presumably by sterically shielding phosphorylated residues from protein phosphatases.

14-3-3 proteins were originally identified 42 years ago as acidic proteins that were highly expressed in the brain [23]. Since then 14-3-3 proteins have been implicated in the regulation of numerous neurological disorders including Parkinson's disease [24, 25]. For example 14-3-3 eta binds to parkin, a protein mutated in autosomal recessive juvenile parkinsonism, and negatively regulates its E3 ligase activity [26]. 14-3-3 proteins interact with alpha-synuclein [27] and have been found in Lewy bodies in brains of patients with Parkinson's disease [28]. Additionally, 14-3-3 theta, epsilon and gamma was recently shown to suppress the toxic effects of alpha-synuclein overexpression in a cell based model of neurotoxicity [29]. Our data suggests that 14-3-3 binding to LRRK2 may be relevant to Parkinson's disease as strikingly 10 out of 41 mutations studied displayed reduced phosphorylation of Ser910/Ser935 and binding to 14-3-3 isoforms (Supplementary Table 1).

How 14-3-3 interaction influences LRRK2 function requires further investigation. Our data suggest that this interaction does not control LRRK2 protein kinase activity, as mutation of Ser910 and/or Ser935 does not influence LRRK2 catalytic activity (Fig 3D). However, our experiments indicate that 14-3-3 binding influences the cytoplasmic localisation of LRRK2, as disruption of 14-3-3 binding by mutation of Ser910/Ser935 caused LRRK2 to accumulate within cytoplasmic pools. Previous work has revealed that LRRK2 mutants including LRRK2[R1441C] and LRRK2[Y1699C] when expressed in cells accumulate within cytoplasmic pools resembling inclusion bodies [9, 19, 30], a finding we were able to confirm

in this study (Fig 7 or supplementary Fig 1). These cytoplasmic pools were suggested to comprise aggregates of misfolded unstable LRRK2 protein [9]. If this were the case it may suggest that 14-3-3 plays a role in stabilising LRRK2. Strikingly, five out of the 6 most common pathogenic mutations (R1441C, R1441G, R1441H, Y1699C and I2020T) accumulated within cytoplasmic pools and displayed reduced Ser910/Ser935 phosphorylation and binding to 14-3-3 under conditions in which wild type LRRK2 and most other LRRK2 mutants analysed bound 14-3-3 and did not accumulate within cytosolic pools (Fig 7). We also validate these findings by demonstrating that Ser910/Ser935 phosphorylation and 14-3-3 binding is markedly reduced in three mouse tissues derived from homozygous R1441C knockin mice that display impaired dopaminergic neurotransmission [20]. Further work is required to establish why the R1441C, R1441G, R1441H, Y1699C and I2020T mutations disrupt phosphorylation of Ser910 and Ser935 hence inhibiting 14-3-3 binding. It is possible that these mutations are partially misfolded or unstable and are hence not properly recognised by the upstream protein kinase that phosphorylates the Ser910 and Ser935 residues.

In Table 1 we subdivide the 41 LRRK2 mutations we have analysed into six groups based on the impact that the mutations analysed in this study have on protein kinase activity, Ser910/Ser935 phosphorylation and14-3-3-binding as well as cellular localisation. Only three out of the 41 mutations analysed markedly enhanced LRRK2 protein kinase two to four-fold. Strikingly, the LRRK2[T2031S] mutation was more active than the LRRK2[G2019S] mutant, displaying nearly 4-fold higher activity than wild type LRRK2. The LRRK2[T2031S] mutation has only been reported in a single Spanish patient with a family history of PD [31]. Interestingly, Thr2031 lies within the T-loop of the LRRK2 kinase domain, a region where many kinases are activated by phosphorylation. Recent studies have suggested that LRRK2 is capable of autophosphorylating itself at Thr2031 [32, 33], although thus far we have thus far never been able to observe detectable phosphorylation of this site in endogenous or overexpressed LRRK2 by mass spectrometry. We have found that changing Thr2031 to Ala to prevent phosphorylation led to a similar increase in activity as the T2031S mutation (RJN data not shown) and mutation to Glu to mimic phosphorylation inactivates LRRK2 (ND data not shown). Further work is warranted to understand the role of Thr2031 and how its mutation to Ser and/or phosphorylation or other covalent modification impacts on LRRK2 catalytic activity. The LRRK2[R1728H] mutation displayed 2-fold increased kinase activity and was identified in a single patient with a family history of PD [6]. The Arg1728 residue is located outside the kinase domain in the COR domain (Fig 5).

In future work it would be important to further investigate how 14-3-3 binding impacts on LRRK2 stability, interaction with substrates or other regulators. It would also be interesting to undertake a more detailed characterisation of the cytoplasmic pools that non-14-3-3 binding LRRK2 mutants accumulate in and to determine whether these do indeed comprise aggregates of misfolded protein. Our results analysing some of the properties of 41 Parkinson's disease associated forms of LRRK2 emphasize that most mutations do not exert their effects in the same way as the G2019S mutation by simply increasing catalytic activity. Finding out how the diverse mutations affect LRRK2 regulation, ability to interact with binding partners and stability as well as downstream functions will provide valuable insights into how LRRK2 exerts its influence in Parkinson's disease. It would also be important to further explore link between of LRRK2-Ser910/Ser935 phosphorylation, 14-3-3 binding and its relevance to development of Parkinson's disease. However, as 28 LRRK2 mutations possessed similar activity, 14-3-3 binding and cellular localisation as wild type LRRK2 there is clearly still much to learn about how the majority of described mutations impact on LRRK2 to cause Parkinson's disease. Finally, it would be interesting to undertake LRRK2

interactor screens from neuronal cell lines or brain tissues that might reveal cofactors other than 14-3-3 that would be relevant to understanding how LRRK2 is regulated and functions.

Acknowledgements

We thank the Sequencing Service (School of Life Sciences, University of Dundee, Scotland) for DNA sequencing, the Post Genomics and Molecular Interactions Centre for Mass Spectrometry facilities (School of Life Sciences, University of Dundee, Scotland) and the protein production and antibody purification teams [Division of Signal Transduction Therapy (DSTT), University of Dundee] co-ordinated by Hilary McLauchlan and James Hastie for purification of antibodies. We would also like to thank Miratul Muqit for helpful discussions. ND is supported by MRCT Industry collaborative award. We thank the Medical Research Council, The Michael J Fox Foundation and the pharmaceutical companies supporting the Division of Signal Transduction Therapy Unit (AstraZeneca, Boehringer-Ingelheim, GlaxoSmithKline, Merck-Serono and Pfizer) for financial support.

References

1 Zimprich, A., Biskup, S., Leitner, P., Lichtner, P., Farrer, M., Lincoln, S., Kachergus, J., Hulihan, M., Uitti, R. J., Calne, D. B., Stoessl, A. J., Pfeiffer, R. F., Patenge, N., Carbajal, I. C., Vieregge, P., Asmus, F., Muller-Myhsok, B., Dickson, D. W., Meitinger, T., Strom, T. M., Wszolek, Z. K. and Gasser, T. (2004) Mutations in LRRK2 cause autosomal-dominant parkinsonism with pleomorphic pathology. Neuron. 44, 601-607

2 Paisan-Ruiz, C., Jain, S., Evans, E. W., Gilks, W. P., Simon, J., van der Brug, M., Lopez de Munain, A., Aparicio, S., Gil, A. M., Khan, N., Johnson, J., Martinez, J. R., Nicholl, D., Carrera, I. M., Pena, A. S., de Silva, R., Lees, A., Marti-Masso, J. F., Perez-Tur, J., Wood, N. W. and Singleton, A. B. (2004) Cloning of the gene containing mutations that cause PARK8-linked Parkinson's disease. Neuron. 44, 595-600

3 Mata, I. F., Wedemeyer, W. J., Farrer, M. J., Taylor, J. P. and Gallo, K. A. (2006) LRRK2 in Parkinson's disease: protein domains and functional insights. Trends Neurosci. 29, 286-293

4 Healy, D. G., Falchi, M., O'Sullivan, S. S., Bonifati, V., Durr, A., Bressman, S., Brice, A., Aasly, J., Zabetian, C. P., Goldwurm, S., Ferreira, J. J., Tolosa, E., Kay, D. M., Klein, C., Williams, D. R., Marras, C., Lang, A. E., Wszolek, Z. K., Berciano, J., Schapira, A. H., Lynch, T., Bhatia, K. P., Gasser, T., Lees, A. J. and Wood, N. W. (2008) Phenotype, genotype, and worldwide genetic penetrance of LRRK2-associated Parkinson's disease: a case-control study. Lancet Neurol. 7, 583-590

5 Biskup, S. and West, A. B. (2008) Zeroing in on LRRK2-linked pathogenic mechanisms in Parkinson's disease. Biochim Biophys Acta

6 Paisan-Ruiz, C., Nath, P., Washecka, N., Gibbs, J. R. and Singleton, A. B. (2008) Comprehensive analysis of LRRK2 in publicly available Parkinson's disease cases and neurologically normal controls. Hum Mutat. 29, 485-490

7 Anand, V. S. and Braithwaite, S. P. (2009) LRRK2 in Parkinson's disease: biochemical functions. FEBS J. 276, 6428-6435

8 West, A. B., Moore, D. J., Biskup, S., Bugayenko, A., Smith, W. W., Ross, C. A., Dawson, V. L. and Dawson, T. M. (2005) Parkinson's disease-associated mutations in leucine-rich repeat kinase 2 augment kinase activity. Proc Natl Acad Sci U S A. 102, 16842-16847

9 Greggio, E., Jain, S., Kingsbury, A., Bandopadhyay, R., Lewis, P., Kaganovich, A., van der Brug, M. P., Beilina, A., Blackinton, J., Thomas, K. J., Ahmad, R., Miller, D. W., Kesavapany, S., Singleton, A., Lees, A., Harvey, R. J., Harvey, K. and Cookson, M. R. (2006) Kinase activity is required for the toxic effects of mutant LRRK2/dardarin. Neurobiol Dis. 23, 329-341

10 Jaleel, M., Nichols, R. J., Deak, M., Campbell, D. G., Gillardon, F., Knebel, A. and Alessi, D. R. (2007) LRRK2 phosphorylates moesin at threonine-558: characterization of how Parkinson's disease mutants affect kinase activity. Biochem J. 405, 307-317

11 Nichols, R. J., Dzamko, N., Hutti, J. E., Cantley, L. C., Deak, M., Moran, J., Bamborough, P., Reith, A. D. and Alessi, D. R. (2009) Substrate specificity and inhibitors of LRRK2, a protein kinase mutated in Parkinson's disease. Biochem J. 424, 47-60

12 Reed, S. E., Staley, E. M., Mayginnes, J. P., Pintel, D. J. and Tullis, G. E. (2006) Transfection of mammalian cells using linear polyethylenimine is a simple and effective means of producing recombinant adeno-associated virus vectors. J Virol Methods. 138, 85-98

13 Dubois, F., Vandermoere, F., Gernez, A., Murphy, J., Toth, R., Chen, S., Geraghty, K. M., Morrice, N. A. and Mackintosh, C. (2009) Differential 14-3-3-affinity capture reveals new downstream targets of PI 3-kinase signaling. Mol Cell Proteomics

14 Moorhead, G., Douglas, P., Cotelle, V., Harthill, J., Morrice, N., Meek, S., Deiting, U., Stitt, M., Scarabel, M., Aitken, A. and MacKintosh, C. (1999) Phosphorylation-dependent interactions between enzymes of plant metabolism and 14-3-3 proteins. Plant J. 18, 1-12
15 Wang, L., Xie, C., Greggio, E., Parisiadou, L., Shim, H., Sun, L., Chandran, J., Lin, X., Lai, C., Yang, W. J., Moore, D. J., Dawson, T. M., Dawson, V. L., Chiosis, G., Cookson, M. R. and Cai, H. (2008) The chaperone activity of heat shock protein 90 is critical for maintaining the stability of leucine-rich repeat kinase 2. J Neurosci. 28, 3384-3391
16 Goransson, O., Deak, M., Wullschleger, S., Morrice, N. A., Prescott, A. R. and Alessi, D. R. (2006) Regulation of the polarity kinases PAR-1/MARK by 14-3-3 interaction and phosphorylation. J Cell Sci. 119, 4059-4070
17 Mackintosh, C. (2004) Dynamic interactions between 14-3-3 proteins and phosphoproteins regulate diverse cellular processes. Biochem J. 381, 329-342
18 Yaffe, M. B., Rittinger, K., Volinia, S., Caron, P. R., Aitken, A., Leffers, H., Gamblin, S. J., Smerdon, S. J. and Cantley, L. C. (1997) The structural basis for 14-3-3:phosphopeptide binding specificity. Cell. 91, 961-971
19 Alegre-Abarrategui, J., Christian, H., Lufino, M. M., Mutihac, R., Venda, L. L., Ansorge, O. and Wade-Martins, R. (2009) LRRK2 regulates autophagic activity and localizes to specific membrane microdomains in a novel human genomic reporter cellular model. Hum Mol Genet. 18, 4022-4034
20 Tong, Y., Pisani, A., Martella, G., Karouani, M., Yamaguchi, H., Pothos, E. N. and Shen, J. (2009) R1441C mutation in LRRK2 impairs dopaminergic neurotransmission in mice. Proc Natl Acad Sci U S A. 106, 14622-14627
21 Hausser, A., Link, G., Hoene, M., Russo, C., Selchow, O. and Pfizenmaier, K. (2006) Phospho-specific binding of 14-3-3 proteins to phosphatidylinositol 4-kinase III beta protects from dephosphorylation and stabilizes lipid kinase activity. J Cell Sci. 119, 3613-3621
22 Hutchins, J. R., Dikovskaya, D. and Clarke, P. R. (2002) Dephosphorylation of the inhibitory phosphorylation site S287 in Xenopus Cdc25C by protein phosphatase-2A is inhibited by 14-3-3 binding. FEBS Lett. 528, 267-271
23 Moore, B. W. and Perez, V. J. (1967) Specific acidic proteins of the nerous system. Pysiological and Biochemical Aspects of Nervous Integration (F.D Carlson, ed). Wood Hole, MA; Prentice-Hall, Inc, 343-359
24 Berg, D., Holzmann, C. and Riess, O. (2003) 14-3-3 proteins in the nervous system. Nat Rev Neurosci. 4, 752-762
25 Chen, H. K., Fernandez-Funez, P., Acevedo, S. F., Lam, Y. C., Kaytor, M. D., Fernandez, M. H., Aitken, A., Skoulakis, E. M., Orr, H. T., Botas, J. and Zoghbi, H. Y. (2003) Interaction of Akt-phosphorylated ataxin-1 with 14-3-3 mediates neurodegeneration in spinocerebellar ataxia type 1. Cell. 113, 457-468
26 Sato, S., Chiba, T., Sakata, E., Kato, K., Mizuno, Y., Hattori, N. and Tanaka, K. (2006) 14-3-3eta is a novel regulator of parkin ubiquitin ligase. EMBO J. 25, 211-221
27 Ostrerova, N., Petrucelli, L., Farrer, M., Mehta, N., Choi, P., Hardy, J. and Wolozin, B. (1999) alpha-Synuclein shares physical and functional homology with 14-3-3 proteins. J Neurosci. 19, 5782-5791
28 Ubl, A., Berg, D., Holzmann, C., Kruger, R., Berger, K., Arzberger, T., Bornemann, A. and Riess, O. (2002) 14-3-3 protein is a component of Lewy bodies in Parkinson's disease-mutation analysis and association studies of 14-3-3 eta. Brain Res Mol Brain Res. 108, 33-39
29 Yacoubian, T. A., Slone, S. R., Harrington, A. J., Hamamichi, S., Schieltz, J. M., Caldwell, G. A. and Standaert, D. G. (2010) Differential neuroprotective effects of 14-3-3 proteins in models of Parkinson's disease. Cell Death and Disease. 1, e2
30 Smith, W. W., Pei, Z., Jiang, H., Moore, D. J., Liang, Y., West, A. B., Dawson, V. L., Dawson, T. M. and Ross, C. A. (2005) Leucine-rich repeat kinase 2 (LRRK2) interacts with

parkin, and mutant LRRK2 induces neuronal degeneration. Proc Natl Acad Sci U S A. 102, 18676-18681

31 Lesage, S., Janin, S., Lohmann, E., Leutenegger, A. L., Leclere, L., Viallet, F., Pollak, P., Durif, F., Thobois, S., Layet, V., Vidailhet, M., Agid, Y., Durr, A., Brice, A., Bonnet, A. M., Borg, M., Broussolle, E., Damier, P., Destee, A., Martinez, M., Penet, C., Rasco, O., Tison, F., Tranchan, C. and Verin, M. (2007) LRRK2 exon 41 mutations in sporadic Parkinson disease in Europeans. Arch Neurol. 64, 425-430

32 Greggio, E., Taymans, J. M., Zhen, E. Y., Ryder, J., Vancraenenbroeck, R., Beilina, A., Sun, P., Deng, J., Jaffe, H., Baekelandt, V., Merchant, K. and Cookson, M. R. (2009) The Parkinson's disease kinase LRRK2 autophosphorylates its GTPase domain at multiple sites. Biochem Biophys Res Commun. 389, 449-454

33 Li, X., Moore, D. J., Xiong, Y., Dawson, T. M. and Dawson, V. L. Reevaluation of phosphorylation sites in the Parkinson's disease associated leucine rich repeat kinase-2. J Biol Chem

34 Cox, J. and Mann, M. (2008) MaxQuant enables high peptide identification rates, individualized p.p.b.-range mass accuracies and proteome-wide protein quantification. Nat Biotechnol. 26, 1367-1372

Figure Legends

Figure 1. **Quantitative mass spectrometry identifies 14-3-3 as an LRRK2-interactor**. HEK-293 cells stably expressing GFP, wild type full-length GFP-LRRK2 or full-length GFP-LRRK2[G2019S] mutant were cultured for multiple passages in either R6K4 SILAC media (GFP-LRRK2) or R10K8 (GFP-LRRK2[G2019S]) or normal R0K0 SILAC media (GFP). Cells were lysed and equal amounts of lysates from GFP and GFP-LRRK2 (A) or GFP and GFP-LRRK2[G2019S] (B) were mixed. Immunoprecipitations were undertaken employing an anti-GFP antibody and electrophoresed on a SDS-polyacrylamide gel, which was stained with colloidal blue (A). Migration of LRRK2 band is indicated with an arrowhead and GFP band is indicated with an arrow. Molecular weights of markers are indicated on the left and right of the gels. The entire lane from each gel was excised, digested with trypsin and processed for mass spectrometry. Each sample was analyzed by Orbitrap mass spectrometry and quantitated using MaxQuant (version 13.13.10) [34] and a summary of results are presented in tabular format. The number of peptides and percent of sequence coverage corresponding to the indicated protein which were quantitated are shown along with the ratios of enrichment for labeled versus unlabeled peptides for each comparison of GFP vs. wild type LRRK2 (A) and GFP vs. LRRK2 [G2019S] (B). The posterior error probability PEP is shown, which measures the accuracy of MaxQuant quantitation where the closer to zero the higher the probability of specific interaction [34].

Figure 2. **Characterisation of 14-3-3 and LRRK2 interaction.** A.) 5 mg of Swiss 3T3 lysate was subjected to immunoprecipitation with control IgG or anti-LRRK2 (S348C) antibody. Immunoprecipitates were subjected to immunoblot analysis with indicated antibodies. B.) 5mg of Swiss 3T3 lysate was subjected to immunoprecipitation with anti-pan 14-3-3 antibodies and immunoprecipitates immunoblotted with indicated antibodies C.) T-Rex HEK 293 cells stably expressing FLAG-LRRK2 [11], were transfected with pEBG plasmids encoding GST or the indicated GST tagged isoform of 14-3-3 and induced to express LRRK2 by inclusion of 1μg/ml of doxycycline in the culture medium. 36 hours post transfection cells were lysed and glutathione-Sepharose affinity purified proteins immunoblotted with indicated antibodies. D.) Endogenous LRRK2 was immunoprecipitated from Swiss 3T3 cells with anti-LRRK2 (S348C) and subsequently treated with λ-phosphatase in the absence or presence of EDTA prior to immunoblot analysis with indicated antibodies or a 14-3-3 overlay assay. E.) As in (D) except experiment undertaken with immunoprecipitated FLAG-LRRK2 obtained following transient transfection in HEK-293 cells.

Figure 3. **Ser910 and Ser935 phosphorylation mediate binding of LRRK2 to 14-3-3**. A.) Endogenous LRRK2 was immunoprecipitated with anti-LRRK2 100-500 (S348C) from Swiss 3T3 cells and FLAG-LRRK2 was immunoprecipitated with anti-FLAG agarose from stable, inducible T-Rex HEK 293 cells. Immunoprecipitates were subjected to electrophoresis on a 4-12% Novex SDS-polyacrylamide gel and stained with colloidal blue. Gel is representative of several experiments. LRRK2 tryptic peptides were subjected to LC-MSMS on an LTQ-Orbitrap mass spectrometer. B.) Phosphopeptides identified by LTQ-Orbitrap mass spectrometry shown in tabular format. Observed mass (m/z) and predicted mass (M) are shown, along with the site of phosphorylation and peptide sequence identified. The number of experiments evaluated (N) is indicated at the top of the column and the number of times, in total, the phosphorylated peptide was identified is indicated. C.) Domain structure of LRRK2 is presented to scale, with amino acid residues indicating domain boundaries indicated. Position of identified phosphorylation sites is shown. D.) The indicated phosphorylation sites identified in A and B were mutated to Ala and transiently expressed in HEK-293 cells.

LRRK2 was immunoprecipitated with FLAG agarose and equal amounts of each protein were probed with FLAG (total) and ability to directly bind 14-3-3 was assessed in an overlay assay. 14-3-3 and Hsp90 co-immunoprecipitation (Co-IP) was determined by immunoblotting the immunoprecipitates with indicated antibodies. Kinase activity was assayed against 30 μM Nictide and specific activity was determined by correcting incorporation of phosphate for protein levels in the immunoprecipitate by quantitative immunoblot using Odyssey LICOR and is presented as counts per minute/LICOR absorbance units (cpm/LICOR AU). The data is the average of a duplicate experiments that was repeated 4 separate times with similar results. E.) Streptavidin-Agarose was conjugated to a biotinylated di-phosphorylated peptide encompassing Ser910 and Ser935 and incubated in the presence or absence of lambda phosphatase in the presence or absence of the EDTA phosphatase inhibitor. The Agarose beads were then incubated with 293 cell lysates and interaction of 14-3-3 was assessed after beads were extensively washed and subjected to 14-3-3 immunoblot analysis. F.) The indicated forms of FLAG-LRRK2 were expressed in 293 cells by transient transfection. 36 h post transfection these were immunoprecipitated with Flag antibody and immunoblotted with phosphospecific antibodies against S910 (S357C) and S935 (S814C). Direct binding of immunoprecipitates to 14-3-3 was also assessed by 14-3-3-overlay assay and co-immunoprecipitation of 14-3-3 and Hsp90 assessed by immunoblotting with the respective antibodies. G.) LRRK2 was immunoprecipitated from tissues of wild type male C57BL/6 mice and immunoblotted for Ser910 and Ser935 phosphorylation and 14-3-3 binding was assessed by overlay assay as in F. H.) Multiple sequence alignment of LRRK2 from Homo sapiens (NP_940980), Pan troglodytes (XP_001168494), Mus musculus (NP_080006), Rattus norvegicus (XP_235581), Bos Taurus (XP_615760), Canis lupis familiaris (XP_543734), and Gallus gallus (XP_427077). Position of the phosphorylated residues Serine 910 and 935 are indicated. Identical residues are indicated in blue. I.) Sequence comparison of residues surrounding the Ser910 and Ser935 phosphorylation sites of human LRRK2.

Figure 4. **14-3-3 binding influences LRRK2 cytoplasmic localisation**. A.) Stable-inducible T-REx cells lines harbouring the indicated forms of LRRK2 were induced for 24 hours with 0.1 μg/ml doxycycline to induce expression of GFP-LRRK2. Equal amount of cell lysate from induced cells of each mutant was subjected to immunoblot analysis with anti-GFP antibodies to detect the fusion protein or anti-GAPDH as a loading control. B.) Fluorescent micrographs representative of cultures of the indicated forms GFP-LRRK2 are shown. Cytoplasmic pools of GFP-LRRK2 observed in the non-14-3-3 binding mutants are indicated with white arrowheads.

Figure 5. **Activity and 14-3-3 Binding of 41 Parkinson's disease associated LRRK2 mutants**. The inset illustrates the domain structure of LRRK2 with the Leucine-Rich Repeats (LRR), Ras of Complex GTPase domain (ROC), Carboxy terminal of Roc (COR), and Kinase catalytic domain (Kinase) and the minimal WD40 repeat domain (WD40) annotated. Positions of the PD associated mutations are shown. The amino acid boundaries of the domains are indicated. The indicated variants of full length FLAG tagged LRRK2 were transiently expressed in HEK 293 cells and subjected to immunoprecipitation analysis. Kinase activity of immunoprecipitates was assessed against LRRKtide and specific activity was determined by quantitative anti-FLAG immunoblot analysis of LRRK2 using LICOR technology and was defined as cpm/LICOR. Wild type LRRK2 activity was set to 1 and the mutant activities are relative to wild type. Assays were performed in duplicate, for three experiments, bars are s.e.m. FLAG-LRRK2 immunoprecipitates were also subjected to immunoblot analysis with anti-FLAG, anti-pSer910 and anti-pSer935 antibodies. 14-3-3

binding to the LRRK2 variants was assessed by 14-3-3 far western analyses and 14-3-3 immunoblotting for co-precipitating 14-3-3.

Figure 6. **Disruption of Ser910/Ser935 phosphorylation and 14-3-3 binding in LRRK2[R1441C] knockin mice**. Brain, kidney and spleen tissue was rapidly excised from three homozygous LRRK2[R1441C] knockin mice and three wild type littermate controls and snap-frozen in liquid nitrogen. LRRK2 was immunoprecipitated from whole tissue lysate of brain, kidney or spleen. Immunoprecipitates were immunoblotted for phosphorylation of LRRK2 at Ser910 and Ser935 and for total LRRK2. Ability to interact with 14-3-3 binding was assessed by 14-3-3 far western analysis. Note insufficient sample from Spleen was available for measuring Ser910 phosphorylation.

Figure 7. **Localisation of 41 PD associated LRRK2 mutants**. Parallel cultures of stable-inducible T-REx cells lines harboring the indicated mutations were induced for 24 hours with 1μg/ml doxycycline to induce expression of GFP-LRRK2. Upper panel, equal amount of cell lysate from induced cells of each mutant was subjected to immunoblot analysis with anti-GFP antibodies to detect the fusion protein or anti-ERK1 as a loading control. Lower panel, fluorescent micrographs representative of cultures of each PD associated mutant (panels 1-43) are shown. Cytoplasmic pools of GFP-LRRK2 are indicated with white arrowheads. Localization analyses were performed in duplicate, on two independently generated stable cell lines. Larger panels of each of the micrographs shown are presented in Supplementary Fig 1.

Biochemical Journal Immediate Publication. Published on 19 Jul 2010 as manuscript BJ20100483

A.

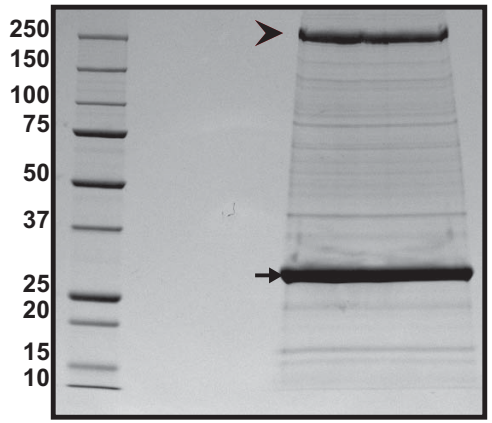

Wild type LRRK2 vs. GFP

wild type LRRK2 vs. GFP Protein Name	Uniprot	Peptides analyzed (#)	Sequence Coverage [%]	Mol. Weight [kDa]	PEP	Ratio H/L
Leucine-rich repeat kinase 2	Q5S007	81	29.7	286.1	0	47.5
14-3-3 zeta/delta	P63104	4	5.7	27.7	6.00E-18	30.8
14-3-3 theta	P27348	7	15.5	27.8	1.05E-31	30.7
14-3-3 epsilon	P62258	6	14.5	29.2	1.57E-39	20.4
14-3-3 beta/alpha	P31946	5	5.7	28.1	7.75E-14	20.4
14-3-3 eta	Q04917	5	5.7	28.2	7.75E-14	20.4
Cdc37 (Hsp90 co-chaperone)	Q16543	2	5.3	44.5	2.67E-22	15.5
Hsp 90-alpha	P07900	29	16.3	98.2	7.23E-161	6.0
Hsp 90-beta	P08238	27	17	83.3	1.73E-134	5.6

B.

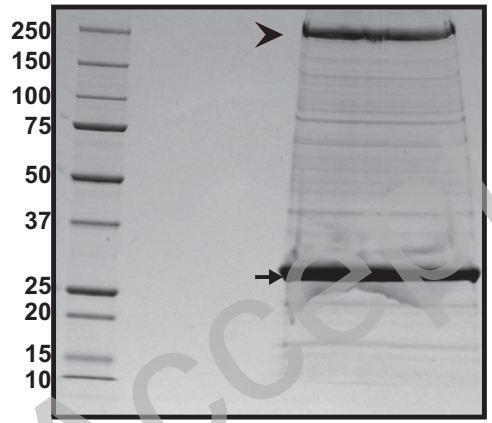

LRRK2 G2019S vs. GFP

LRRK2 [G2019S] vs. GFP Protein Name	Uniprot	Peptides analyzed	Sequence Coverage [%]	Mol. Weight [kDa]	PEP	Ratio H/L
Leucine-rich repeat kinase 2	Q5S007	86	29.7	286.1	0	47.5
14-3-3 theta	P27348	6	15.5	27.8	3.58E-42	13.2
14-3-3 beta/alpha	P31946	4	5.7	28.1	1.98E-15	13.2
14-3-3 zeta/delta	P63104	4	5.7	27.7	7.27E-22	12.8
14-3-3 gamma	P61981	4	4	28.3	3.89E-14	12.0
14-3-3 epsilon	P62258	6	14.1	29.2	1.48E-28	10.9
Cdc37 (Hsp90 co-chaperone)	Q16543	6	18.5	44.5	1.09E-30	8.1
Hsp 90-alpha	P07900	32	19.3	98.2	3.77E-245	5.1
Hsp 90-beta	P08238	32	20.9	83.3	1.47E-200	4.9

Figure 1.

Biochemical Journal Immediate Publication. Published on 19 Jul 2010 as manuscript BJ20100483

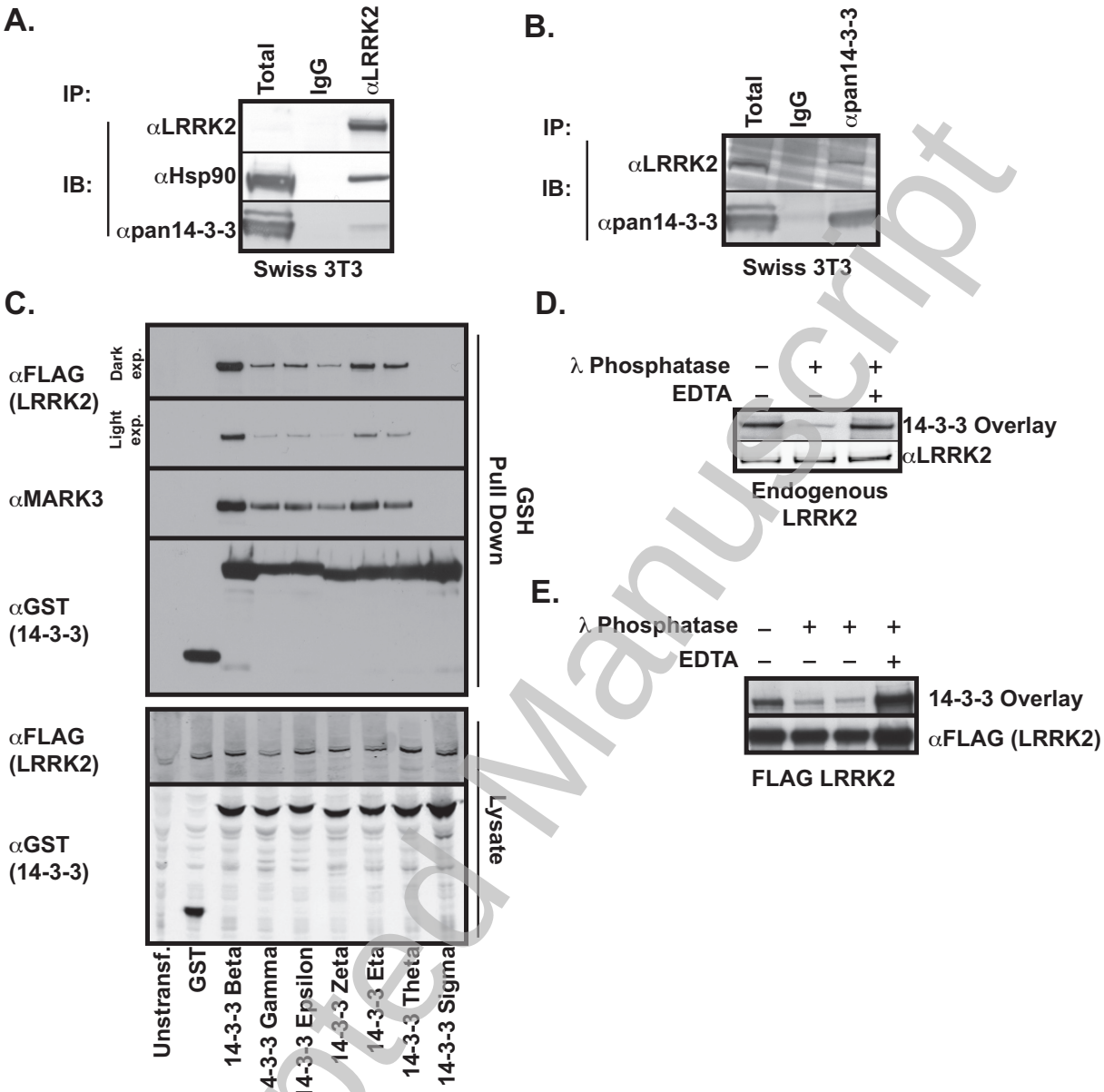

Figure 2.

Biochemical Journal Immediate Publication. Published on 19 Jul 2010 as manuscript BJ20100483

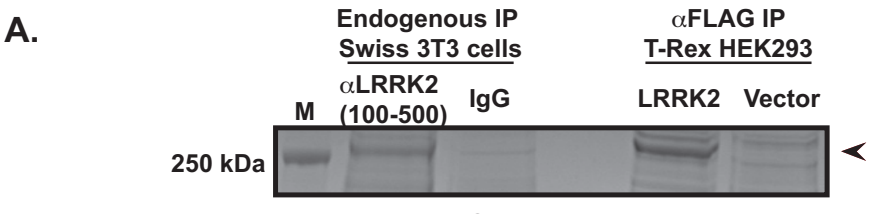

B.

Endogenous LRRK2 Phosphopeptide Analysis (Swiss 3T3 cells)

Mass (m/z)	Mass (M)	Phosphorylated Residue	Sequence	Identified from mouse LRRK2(N=2)
1145.499	2288.9797	860	NTLQEGVASGpSDGNFSEDALAK	1
645.803	1289.5652	910	SNpSISVGEVYR	2
709.852	1417.6602	910	KSNpSISVGEVYR	2
639.307	1914.8625	935	HSNpSLGPVFDHEDLLR	1

FLAG LRRK2 Phosphopeptide Analysis (HEK 293 cells)

Mass (m/z)	Mass (M)	Phosphorylated Residue	Sequence	Identified from human LRRK2 (N=7)
1133.475	2264.9321	860	SAVEEGTASGpSDGNFSEDVLSK	1
669.79	1337.5652	910	SNpSISVGEFYR	4
733.838	1465.6602	910	KSNpSISVGEFYR	4
686.999	2056.9731	935	HSNpSLGPIFDHEDLLKR	1
543.247	1084.4801	955	ILSpSDDSLR	4
684.793	1367.5718	973	HSDpSISSLASER	3
724.777	1447.5381	973/976	HSDpSISpSLASER	2

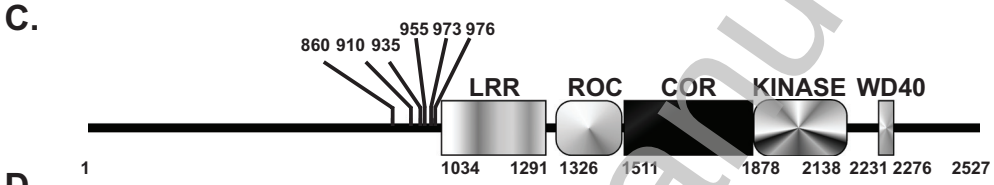

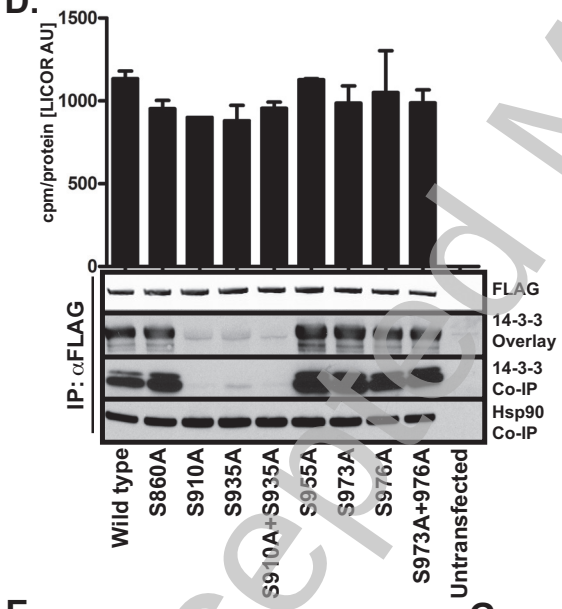

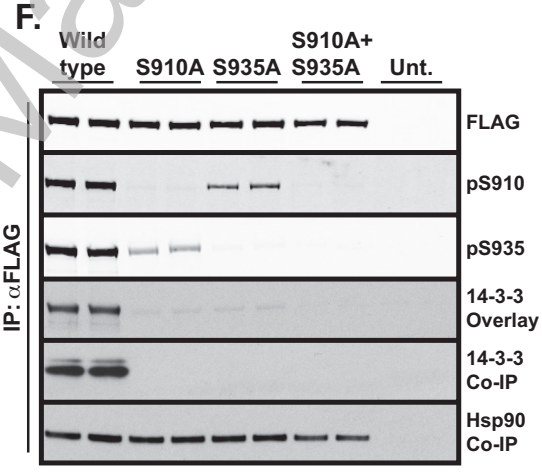

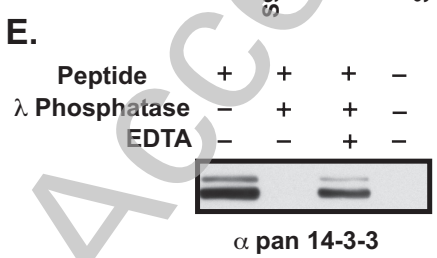

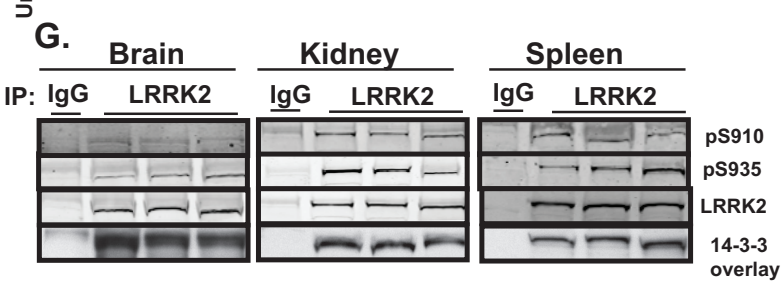

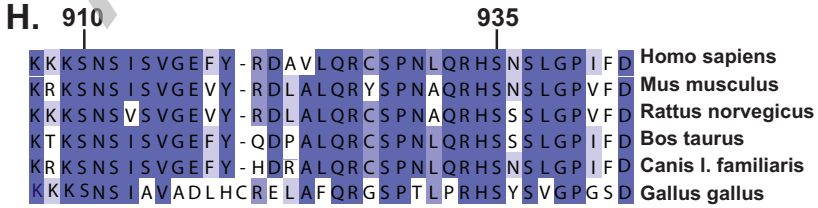

I.

Human Ser910 VKKKSN**S**ISVGEF
Human Ser935 LQRHSN**S**LGPIFD

Figure 3.

Biochemical Journal Immediate Publication. Published on 19 Jul 2010 as manuscript BJ20100483

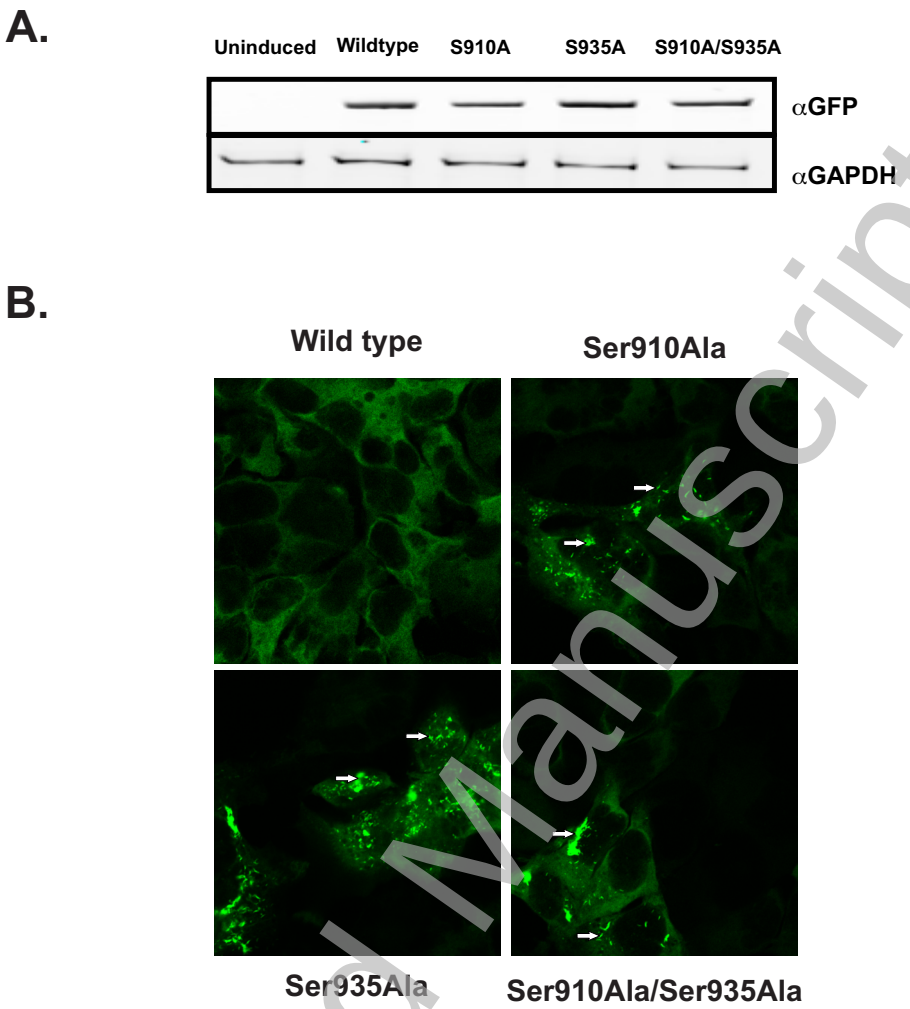

Figure 4

Biochemical Journal Immediate Publication. Published on 19 Jul 2010 as manuscript BJ20100483

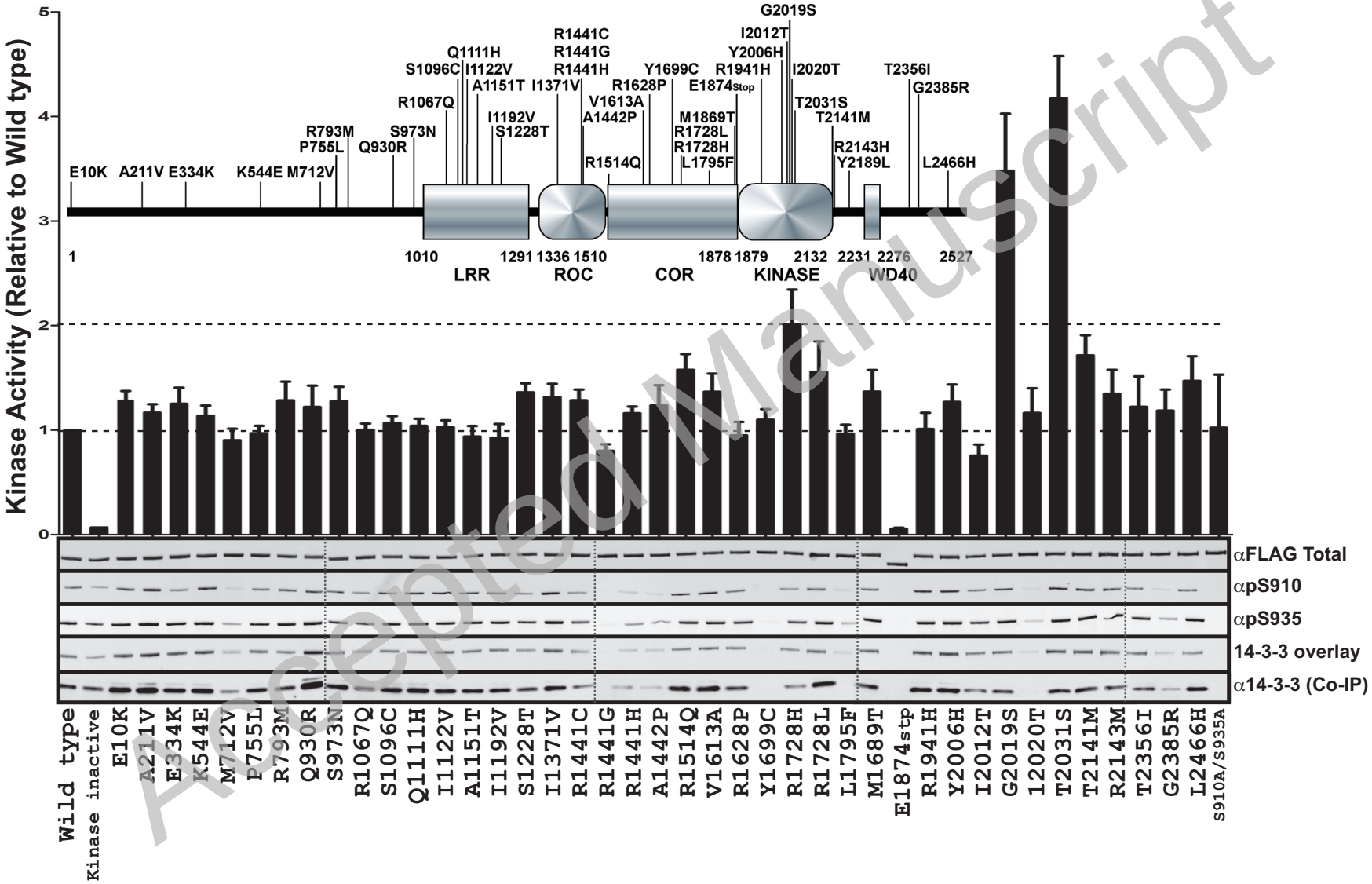

Figure 5

Biochemical Journal Immediate Publication. Published on 19 Jul 2010 as manuscript BJ20100483

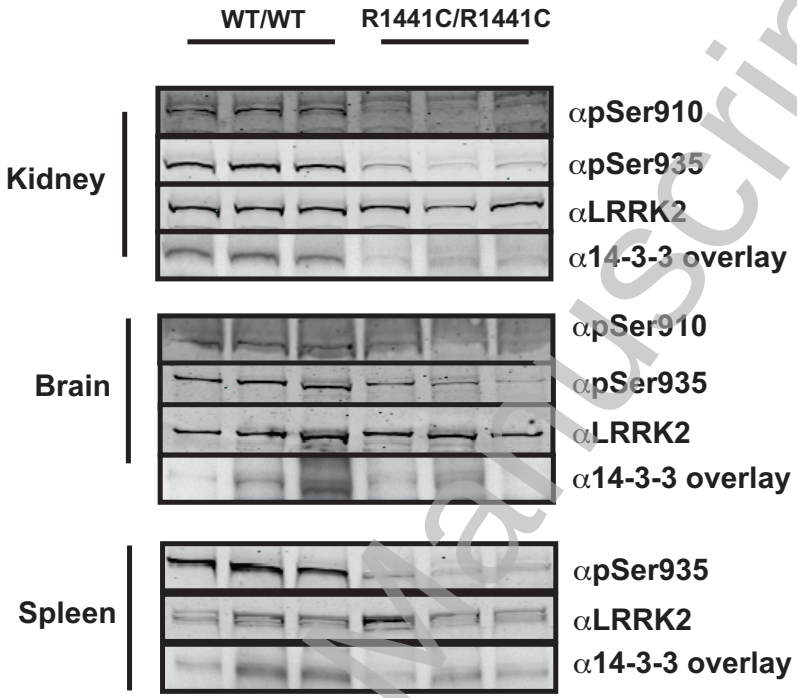

Figure 6.

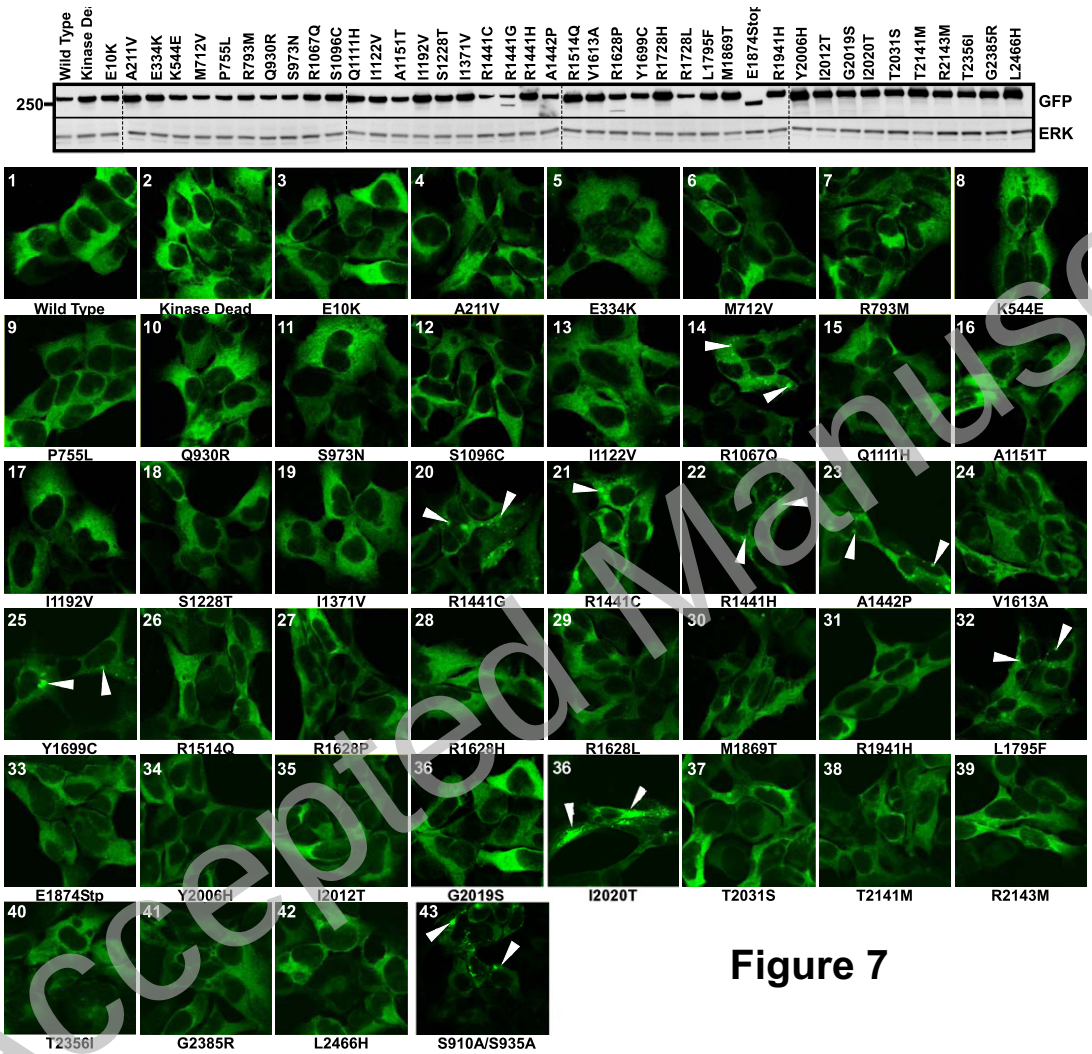

Figure 7